ARMY RESEARCH LABORATORY

Conceptual Aerodynamic Modeling of a Flapping Wing Unmanned Aerial Vehicle

by Justin Alexander Yang

ARL-TR-6747 **November 2013**

Approved for public release; distribution unlimited.

NOTICES

Disclaimers

The findings in this report are not to be construed as an official Department of the Army position unless so designated by other authorized documents.

Citation of manufacturer's or trade names does not constitute an official endorsement or approval of the use thereof.

Destroy this report when it is no longer needed. Do not return it to the originator.

Army Research Laboratory
Aberdeen Proving Ground, MD 21005

ARL-TR-6747 **November 2013**

Conceptual Aerodynamic Modeling of a Flapping Wing Unmanned Aerial Vehicle

Justin Alexander Yang
Vehicle Technology Directorate, ARL

Approved for public release; distribution unlimited.

REPORT DOCUMENTATION PAGE

Form Approved
OMB No. 0704-0188

Public reporting burden for this collection of information is estimated to average 1 hour per response, including the time for reviewing instructions, searching existing data sources, gathering and maintaining the data needed, and completing and reviewing the collection information. Send comments regarding this burden estimate or any other aspect of this collection of information, including suggestions for reducing the burden, to Department of Defense, Washington Headquarters Services, Directorate for Information Operations and Reports (0704-0188), 1215 Jefferson Davis Highway, Suite 1204, Arlington, VA 22202-4302. Respondents should be aware that notwithstanding any other provision of law, no person shall be subject to any penalty for failing to comply with a collection of information if it does not display a currently valid OMB control number.
PLEASE DO NOT RETURN YOUR FORM TO THE ABOVE ADDRESS.

1. **REPORT DATE** *(DD-MM-YYYY)*	**2. REPORT TYPE**	**3. DATES COVERED (From - To)**
November 2013	Final	June to August 2013

4. TITLE AND SUBTITLE
Conceptual Aerodynamic Modeling of a Flapping Wing Unmanned Aerial Vehicle

5a. CONTRACT NUMBER

5b. GRANT NUMBER

5c. PROGRAM ELEMENT NUMBER

6. AUTHOR(S)
Justin Alexander Yang

5d. PROJECT NUMBER

5e. TASK NUMBER

5f. WORK UNIT NUMBER

7. PERFORMING ORGANIZATION NAME(S) AND ADDRESS(ES)
U.S. Army Research Laboratory
ATTN: RDRL-VTV
Aberdeen Proving Ground, MD 21005

8. PERFORMING ORGANIZATION REPORT NUMBER
ARL-TR-6747

9. SPONSORING/MONITORING AGENCY NAME(S) AND ADDRESS(ES)

10. SPONSOR/MONITOR'S ACRONYM(S)

11. SPONSOR/MONITOR'S REPORT NUMBER(S)

12. DISTRIBUTION/AVAILABILITY STATEMENT
Approved for public release; distribution unlimited.

13. SUPPLEMENTARY NOTES
John.w.gerdes.civ@mail.mil

14. ABSTRACT

This report presents the development of an improved aerodynamic model of a flapping wing unmanned aerial vehicle (FWUAV). Flapping wing flight is a complex phenomenon encompassing unsteady effects, controls using multiple degrees of freedom, creation of leading edge vortices, significant wing deformation, and extreme angles of attack during flight. These phenomena are not well modeled using the traditional conceptual aerodynamic models originally developed for fixed wing and rotary wing aircraft. In this study, Blade Element Theory is combined with momentum theory (called Blade Element Momentum Theory [BEMT]) to estimate aerodynamic loads on a FWUAV. The BEMT model is also combined with experimental scans of a FWUAV wing in a wind tunnel to represent the actual wing shape during flight (represented by three-dimensional [3D] scatter plots). These scatter plots are translated into spanwise-changing airfoil coordinates and used with thin airfoil theory to estimate the lift coefficient of the wing across the entire span at discrete points in the flap cycle. Finally, this lift coefficient estimation is used in conjunction with BEMT to create a comprehensive model for flapping wing flight and model calculations are compared against experimental data.

15. SUBJECT TERMS
UAV, flapping, wing, aerial, vehicle, aerodynamic

16. SECURITY CLASSIFICATION OF:			**17. LIMITATION OF ABSTRACT**	**18. NUMBER OF PAGES**	**19a. NAME OF RESPONSIBLE PERSON**
a. REPORT	**b. ABSTRACT**	**c. THIS PAGE**			John W. Gerdes
Unclassified	Unclassified	Unclassified	UU	26	**19b. TELEPHONE NUMBER** (*Include area code*) (410) 278-8735

Standard Form 298 (Rev. 8/98)
Prescribed by ANSI Std. Z39.18

Contents

List of Figures

List of Tables

Acknowledgments

I would like to thank Mr. John Gerdes for his guidance and for introducing me to an exciting new area of research, with which I had absolutely no prior familiarity. Additionally, I'd like to thank Mr. Eric Spero for helping to bring me out to the U.S. Army Research Laboratory (ARL) and Mrs. Deborah Stowell for going above and beyond to help me and all the other summer students with just about everything.

Student Bio

Justin Alexander Yang is a second-year graduate student at the Georgia Institute of Technology, working on his M.S. in aerospace engineering in the Aerospace Systems Design Lab. He is interested in the usage of systems engineering in engineering design, specifically as applied to aerospace and defense. He earned a B.S. in aerospace engineering from the University of Arizona and thinks nothing in the world compares to a Tucson sunset. Yang plans to enter the defense industry upon graduation from Georgia Tech.

1. Introduction/Background

The phenomenon of flapping wing flight in nature has been studied for centuries. Recently, flapping flight for unmanned aerial vehicle (UAV) applications has become an area of interest for military and civilian applications alike. Flapping wing flight offers many potential advantages over traditional fixed and rotary wing aircraft. Fixed wing UAVs are a tried and true platform in theater, with platforms such as the MQ-1 Predator, the RQ-11 Raven, and the RQ-7 Shadow—all of which are currently in use by the U.S. military. These fixed wing vehicles have the advantages of long range and endurance, and high payload capabilities; however, they require high forward flight speeds and most configurations cannot hover, which makes them difficult to control in confined spaces.

Conversely, rotary wing UAVs are highly maneuverable, can fly at lower forward speeds, and can hover, but generally have lower endurance times and are louder than fixed wing UAVs due to high rotor tip speeds. The goal of using flapping wing UAVs (FWUAVs) is to bridge the gap between fixed and rotary wing UAVs. FWUAVs have the potential to fly at lower airspeeds than fixed wing aircraft and most have the ability to hover, which enables FWUAVs to be flown in confined spaces. Compared to rotorcraft, FWUAVs tend to be quieter since the wing flapping speed is generally much slower than a rotor's rotation. This combination of maneuverability, hover capability, and stealthiness makes FWUAVs a potential choice for use in confined spaces. Figure 1 shows an example of each type of UAV.

Figure 1. An example of each types of UAV: (left to right) fixed wing UAV (*1*), rotary wing UAV (*2*), and FWUAV (*1*).

Two main configurations of FWUAVs are currently being investigated: bird-inspired and insect-inspired flight. Bird-inspired flight is based on the forward posture of birds, where a forward velocity is required to maintain lift and the flapping motion is in a roughly vertical plane with respect to the forward velocity. Conversely, insect-inspired flight is characterized by a hovering posture, where insects' wings oscillate in a plane horizontal to the ground. At the beginning and end of each stroke (flap), insect wings will rotate, as shown in figure 2.

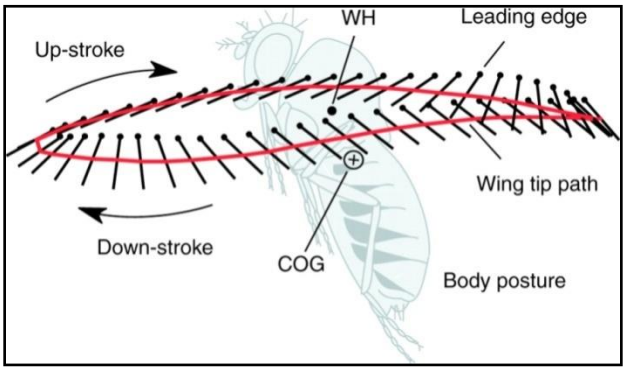

Figure 2. Insect flapping (*3*).

This project is based on the bird-inspired FWUAV called the RoboRaven (figure 3), which was design and built by researchers at the University of Maryland (UMD) (*4*). It has a wingspan of 0.9 m and a max chord length of ~0.3 m. The wings can move independently of one another, driven by two separate servos, which rotate the wings at approximately 3–4 Hz. In flight, the RoboRaven cruises at approximately 6.7 m/s, which is in the flight regime of Reynolds number ~120,000.

Figure 3. UMD RoboRaven.

The overall goal of this project is to improve upon the accuracy of existing FWUAV aerodynamic models to be used in the conceptual design process. FWUAV design is currently a sequential trial and error process, where engineers iterate through many different designs until reaching a desirable configuration. This process is very labor and time intensive, since designers must physically build and test every component on the FWUAV. Aerodynamic models that can accurately predict flight forces enable designers to run through many iterations of design prior to building any prototypes. Additionally, pairing the electric motor that will move the FWUAV's wings to the flapping cycle and flight forces is very important to efficient operation in an FWUAV. Integrating these two fields earlier in the design could potentially yield improved designs and shorter design times.

In order to accomplish the objectives outlined, two main goals were identified:

1. Implement Blade Element Momentum Theory (BEMT) in the J.D. DeLaurier Blade Element Theory flapping wing aerodynamic code (5).
2. Use wing shape data from Digital Image Correlation (DIC) tunnel experiments of an actual RoboRaven UAV to calculate lift coefficient across the UAV wing span:
    a. Use thin airfoil theory to calculate the lift coefficient (C_l)

The above-mentioned BEMT aerodynamic analysis is created using a combination of two aerodynamic theories: Blade Element Theory (BET) and momentum theory. In BET, the wing of a UAV is discretized across the entire span into chordwise "slices." Each of these slices experiences the flight forces of lift, drag, and thrust (in differential form). Because the wing is three dimensional (3-D), each slice is really a small section with a width in the spanwise direction; however, it is treated as an airfoil with infinite span. Once all the differential forces have been calculated at each slice, integration is performed along the entire span to calculate the total forces on the wing, as shown in figure 4.

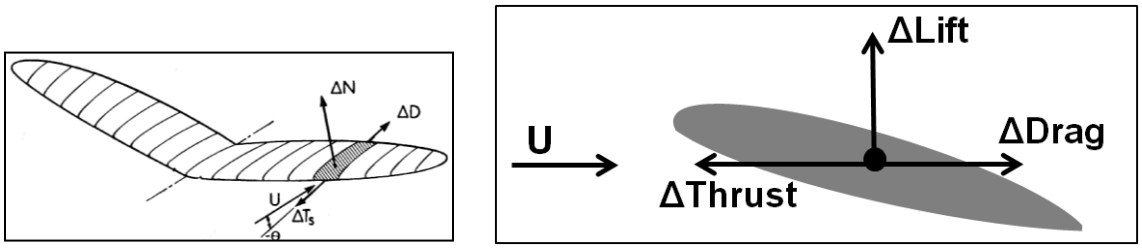

Figure 4. (Left) Discretize wing (5) and wing slide forces.

Compared to BET, momentum theory (figure 5) is a much more simplified approach to calculating aerodynamic forces. In momentum theory, the momentum change of moving air deflected off a wing is used to calculate lift and thrust. When a wing is placed at an angle of attack, α, with respect to the forward velocity, U, it will deflect air downward at a velocity, w, called induced velocity. Induced velocity is ultimately used in momentum theory to calculate lift and thrust.

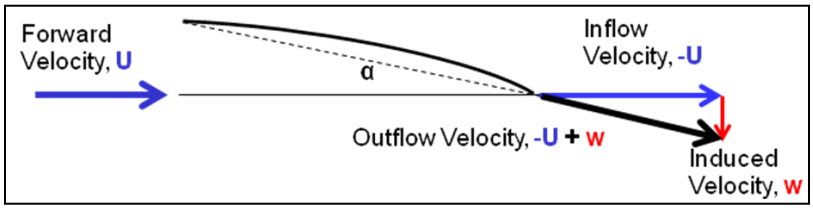

Figure 5. Momentum theory induced velocity.

For a flapping wing, momentum theory analyzes the wings as a "partial actuator disk" (figure 6), where the disk's size is determined by the swept area of the wing flapping when viewing the UAV's frontal area. The momentum change of the air moving across this partial disk area is used to calculate thrust. Thus, in momentum theory, the entire wing flapping motion is represented by the partial disk area, as opposed to discretizing the wing along the span as in BET.

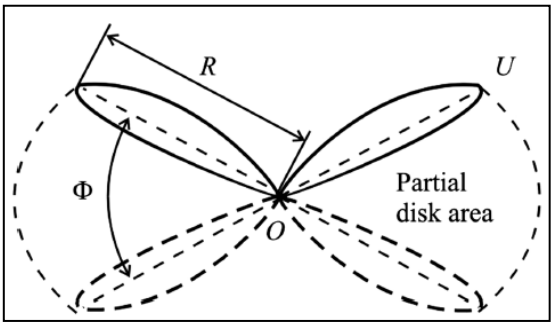

Figure 6. Momentum theory partial disk area (adapted from Shkarayev and Silin [*6*]).

In both BET and momentum theory, there is one unknown variable, induced velocity, in the equations used for thrust calculation (see figure 5). When BET and momentum theory are used separately, induced velocity is either approximated using a function or is assigned a constant value as defined by the individual performing the aerodynamic analysis. BEMT solves this problem by combining the two equations for BET and momentum theory in order to solve for downwash velocity. Once downwash velocity is calculated, it is used in the BET analysis at each spanwise "slice" and forces are calculated.

In the DeLaurier flapping wing BET model (*5*), the lift coefficient is calculated using a function approximation; however, throughout the flapping cycle, a FWUAV's wing shape will change dramatically. It is necessary to account for these shape changes in an aerodynamic modeling code, because wing shape is extremely important when calculating the lift coefficient. In order to account for these shape changes, DIC can be used to measure wing deformation of a FWUAV wing in a wind tunnel. DIC uses high resolution pictures of a patterned wing surface to track movements while the wing is flapping. DIC images of the RoboRaven (taken by UMD researchers [*4*]) throughout the flap cycle offer a snapshot of the wing shape, represented as a scatter plot of the wing (figure 7).

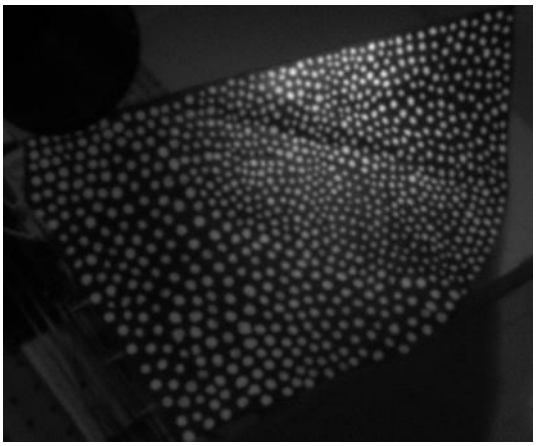

Figure 7. DIC wing covered in markers (*4*).

2. Experiment/Calculations

The experimental phase of this project was completed entirely via computer modeling in MATLAB, thus the following section describes the equations and background for implementing the modeling process. It is divided into two sections, following the two main goals outlined in the background section: creation of the blade element momentum theory model and use of 3-D wing scatter plots with thin airfoil theory to calculate the lift coefficient.

2.1 Blade Element Momentum Theory Model Creation

As described in section 1, the purpose of combining BET and momentum theory is to calculate induced velocity using the two theories together, as opposed to using a functional approximation of induced velocity. J.D. DeLaurier's BET model was used as a basis for creating the BEMT model in this project, in which induced velocity is approximated using

$$\frac{w_0}{U} = \frac{2(\alpha_0 + \bar{\theta})}{2 + AR} \tag{1}$$

(1)

where U = free stream velocity, α_0 = zero lift angle, $\bar{\theta}$ = flight path angle, and AR = aspect ratio.

In this project, BEMT is used to improve upon DeLaurier's induced velocity approximation by integrating the momentum model from Shkarayev and Silin's 2010 paper (*6*) with DeLaurier's BET model. Shkarayev's momentum model estimates the thrust of an FWUAV by examining the air moving through the plane of wing flapping, called a "partial disk area" (see figure 6). It is assumed that the flow through the partial disk area is uniform throughout. The partial disk area is defined by the flap angle, Φ, and wing span, b, according to equation 2. One shortcoming of this

approach is that the flow is not uniform throughout the disk, as flow velocity is highly dependent on wing shape and spanwise position during flapping. A potential improved approach is described in section 4, where future work is presented.

$$A = \frac{\Phi b^2}{4} \tag{2}$$

Using the inputs seen in equation 3 and described below, Shkarayev's momentum theory equation will approximate either induced velocity, if thrust is known, or thrust, if the induced velocity is input. Since it is desired to find a value for the induced velocity to be used in the BET analysis, thrust must be found through another means. This is accomplished in the BEMT model creation procedure, which is described below.

The iteration procedure consists of estimating thrust, using an initial "guess" for the thrust of the FWUAV (figure 8). This thrust estimate is used to calculate induced velocity in equation 3 from Shkarayev and Silin's paper (*6*):

$$w^4 + 2w^3 V cos(\beta) + w^2 V^2 = \left(\frac{T}{2\rho A}\right)^2, \tag{3}$$

where w = induced velocity, V = flight velocity, β = angle of attack, T = thrust, ρ = air density, and A = wing partial disk area.

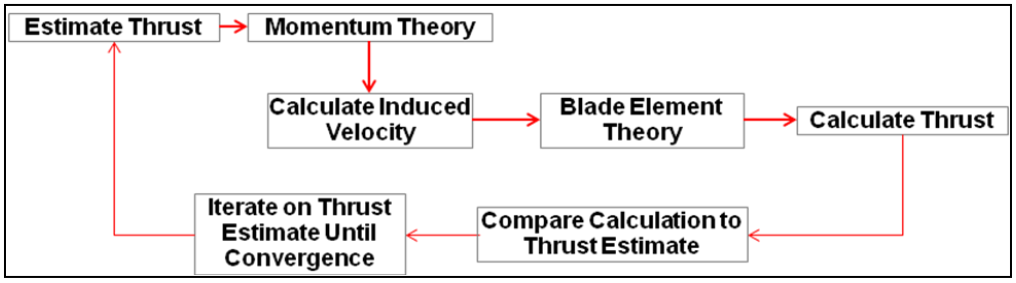

Figure 8. BEMT iteration loop.

Once an initial calculation for induced velocity from momentum theory is obtained, it is used in the original DeLaurier BET code in place of the induced velocity function approximation shown in equation 3. The BET code is used to calculate thrust, and this thrust is compared to the original thrust estimate. Depending on the optimization routine used in this iteration loop, the thrust estimate is systematically modified until the error between the BET calculated thrust and the estimated thrust is minimized. This iteration loop should result in agreement between momentum theory and BET, where the induced velocity estimate used in momentum theory and BET will result in the smallest error between both methods.

2.2 DIC Wing Shape Measurements

As described previously, a FWUAV's wing shape will vary greatly throughout the flap cycle, and the lift coefficient is highly dependent on the wing shape. Thus, it is important to capture wing shape changes during flapping in order to have an accurate representation of the lift coefficient. This project accomplishes the goal of calculating the lift coefficient based on wing shape through the use of DIC wing deformation scatter plots, an example of which is seen in figure 9. These scatter plots are simple 3-D representations of the wing, taken directly from DIC images of an FWUAV flapping in a wind tunnel.

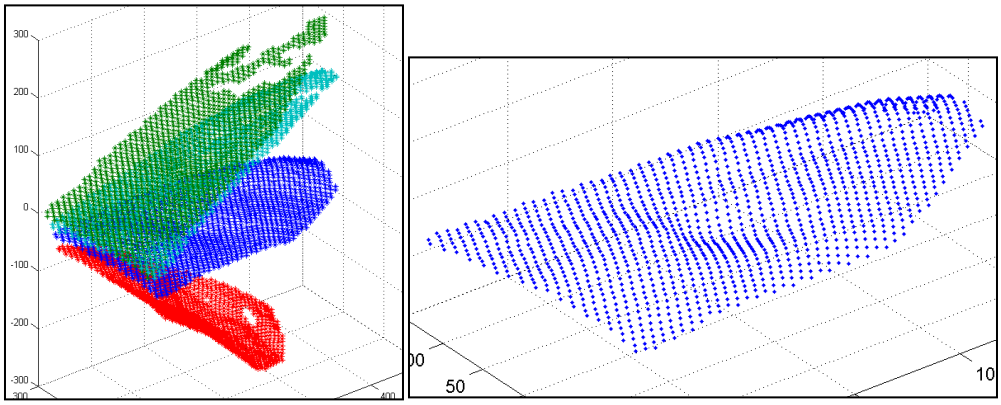

Figure 9. (Left) The 3-D wing scatter plots throughout flap cycle and (right) a 3-D wing scatter plot.

Once the 3-D wing shape scatter plots have been obtained from DIC images, it is necessary to calculate the lift coefficient to be used in BET portion of the BEMT code. In BET, the wing is represented by "slices" along the span, thus it is necessary to calculate the lift coefficient at each of these spanwise slices (figure 10).

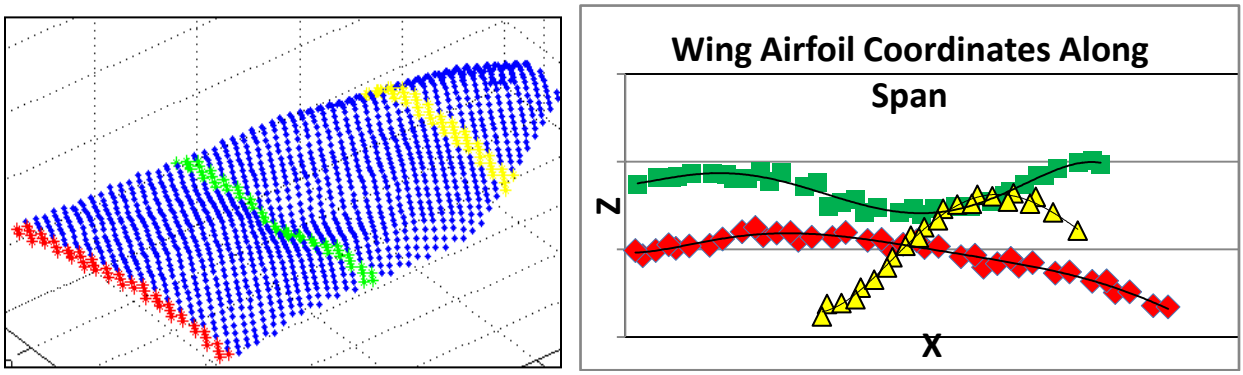

Figure 10. (Left) Wing chord shapes along the span and (right) two-dimensional (2-D) airfoil shapes from the 3-D wing scatter plots.

One method of estimating the lift coefficient is through the use of thin airfoil theory, which calculates C_l using a polynomial approximation of airfoil shape. C_l is calculated according to

equation 4 from Anderson (*7*), where α = angle of attack, dz/dx = derivative of polynomial approximation of wing shape, and θ = chordwise location of airfoil in polar coordinates. The integral shown is in terms of polar coordinates, where one will integrate from the leading edge of the airfoil to the trailing edge of the airfoil, or 0 chord length to 1 chord length. Since the equation is converted to polar coordinates, the bounds become 0 to π. Further explanation can be found in Anderson (*7*).

$$c_l = 2\pi[\alpha + \frac{1}{\pi}\int_0^{\pi} \frac{dz}{dx}(\cos\theta - 1)d\theta] \tag{4}$$

In order to use thin airfoil theory, it is necessary to convert from 3-D wing scatter plots to discrete airfoils along the span, where the airfoils are approximated by a polynomial function, z(x) (figure 11). This was accomplished by grouping wing section slices from 3-D scatter plots along the span into 2-D airfoil shapes, as seen in the chart in figure 11. Depending on the number of slices (e.g., 10), the wing would be split into equal parts along the span. Each of these groups of points is then viewed solely in two dimensions such that the wing shape is seen as a 2-D airfoil. Thus, each spanwise wing section is represented as a simple 2-D airfoil, which is then used in conjunction with thin airfoil theory.

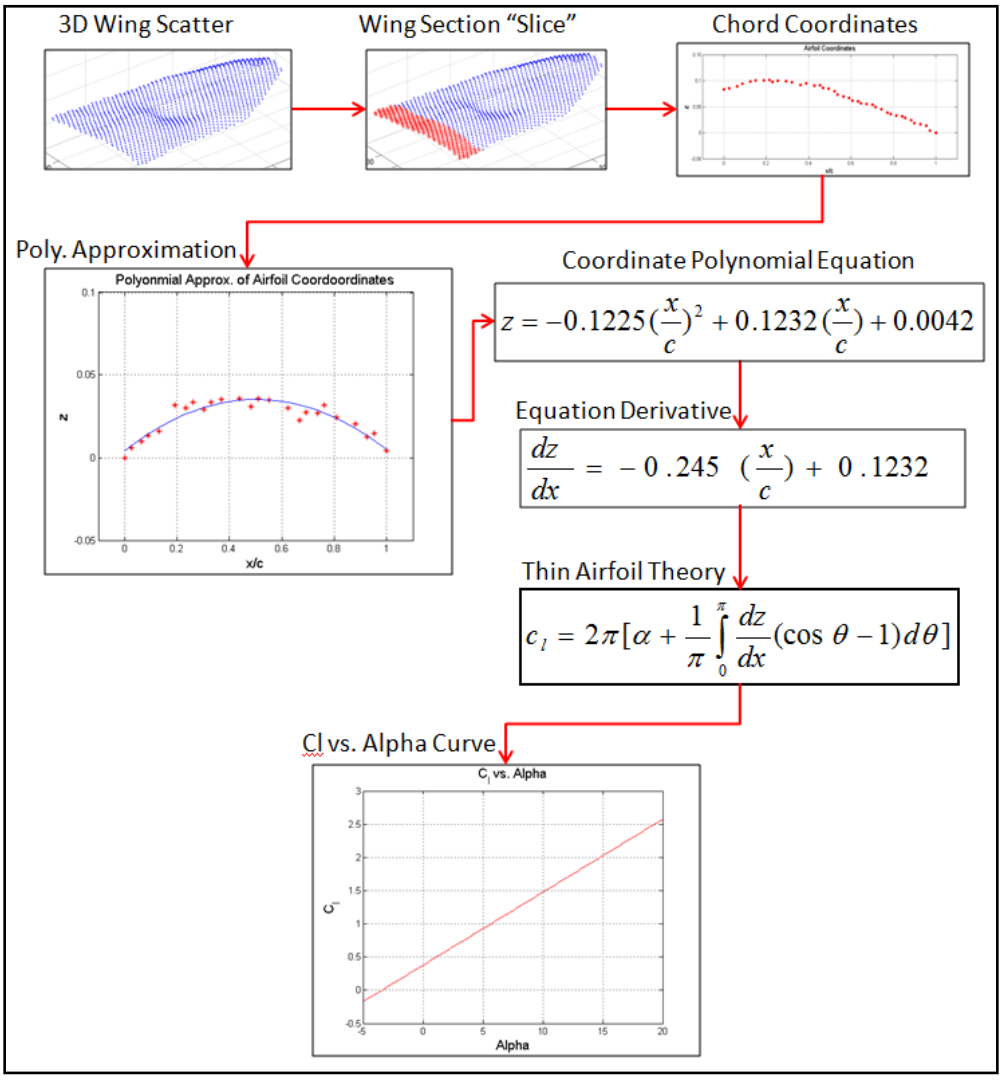

Figure 11. Thin airfoil theory C_l calculation from a 3-D wing scatter plot.

3. Results and Discussion

3.1 BEMT Code Creation

The first phase of the project was to implement BEMT using a combination of the DeLaurier BET code and the Shkarayev momentum theory. In the original DeLaurier paper, a model pterosaur is used as an example for running the code. The pterosaur's geometric properties are provided as inputs, such as wing planform shape and span, as well as flapping cycle properties such as amplitude of flap angle and flapping speed. In the code, the amount of "β = dynamic twist" (wing twisting along the span) was used for analysis, where a more dynamic twist equates

to more twisting along the wing span. As the dynamic twist was changed, the resulting lift and thrust were analyzed. The complete set of inputs can be seen in the DeLaurier paper (*5*); however, in order to compare the BEMT code to the original DeLaurier BET code, these same inputs were used in the BEMT analysis. A comparison of the two is shown in figure 12.

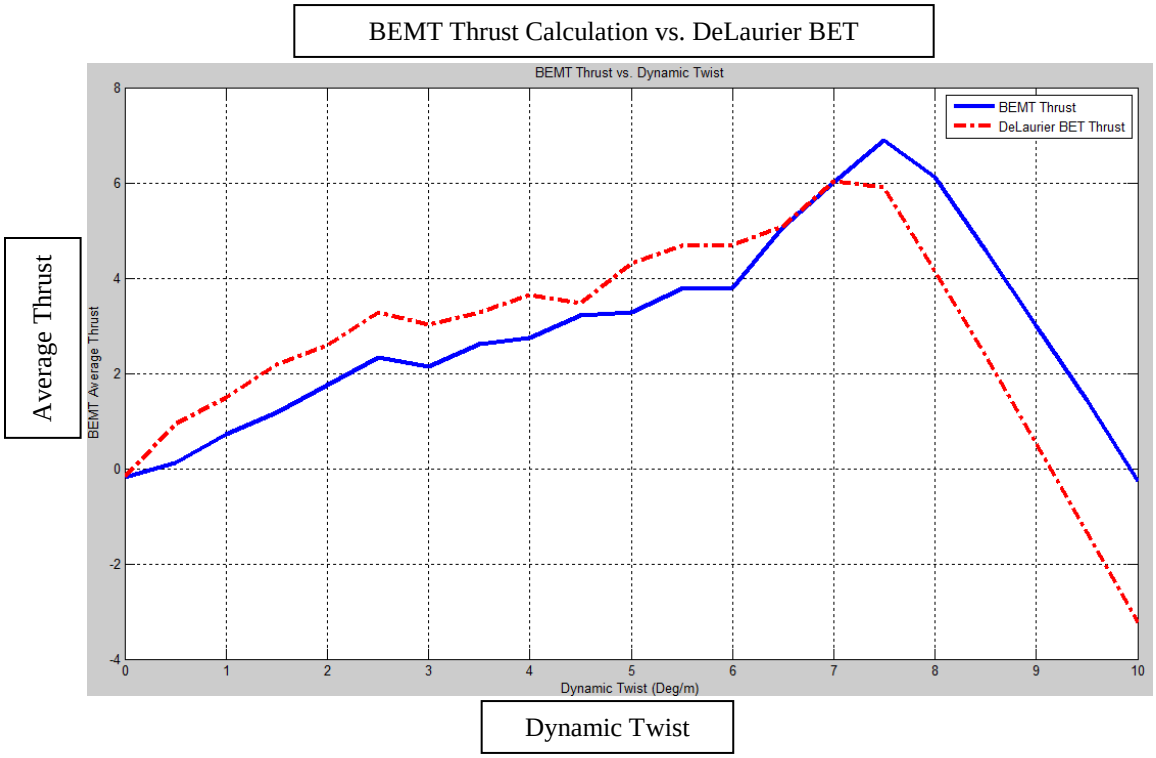

Figure 12. BEMT thrust vs. DeLaurier BET using DeLaurier paper (*5*) inputs.

It is seen that, for the same set of inputs, the DeLaurier BET model overestimates thrust for dynamic twist values of $0 < \beta < 7°/m$, while the BEMT model calculates higher values of thrust for a dynamic twist of $\beta > 7°/m$. It is difficult to draw direct conclusions from the specific values of thrust in this chart, since the input β is not a real geometric input (e.g., not span, chord, etc.) and is only used to estimate the amount of wing twist. However, it can be seen that implementation of BEMT still follows the same trends when using the same set of inputs as the DeLaurier model, which verifies that the BEMT model is behaving "correctly" (assuming the original DeLaurier model was correctly validated).

The above plot of BEMT-calculated thrust versus dynamic twist shows the thrust values converged upon between momentum theory and the DeLaurier BET model in the loop shown in figure 13. These converged values come from the minimum error between BET-calculated thrust and estimated thrust used in momentum theory. Convergence of this BEMT loop was treated as a minimization or optimization problem, where error is a function that must be minimized.

$$Error = (Calculated\ Thrust)_{BET} - Estimated\ Thrust \quad (5)$$

Many optimization algorithms exist; however, in order to save time on implementing a more advanced optimization routine, the approach in this project was simply to use a direct search method. In direct search method algorithms, the function is evaluated using multiple inputs over a specified range, and the resulting minimum-value output is known to be the optimum. A plot of convergence upon the thrust value in the BEMT loop is shown in figure 13. It is seen that the error function is nonlinear and contains multiple local minima; when searching for the global minimum of a function, multiple local minima can cause the optimization algorithm to converge on a local minima should the incorrect input range be used (function inputs bounded around a local minima as opposed to the global minimum).

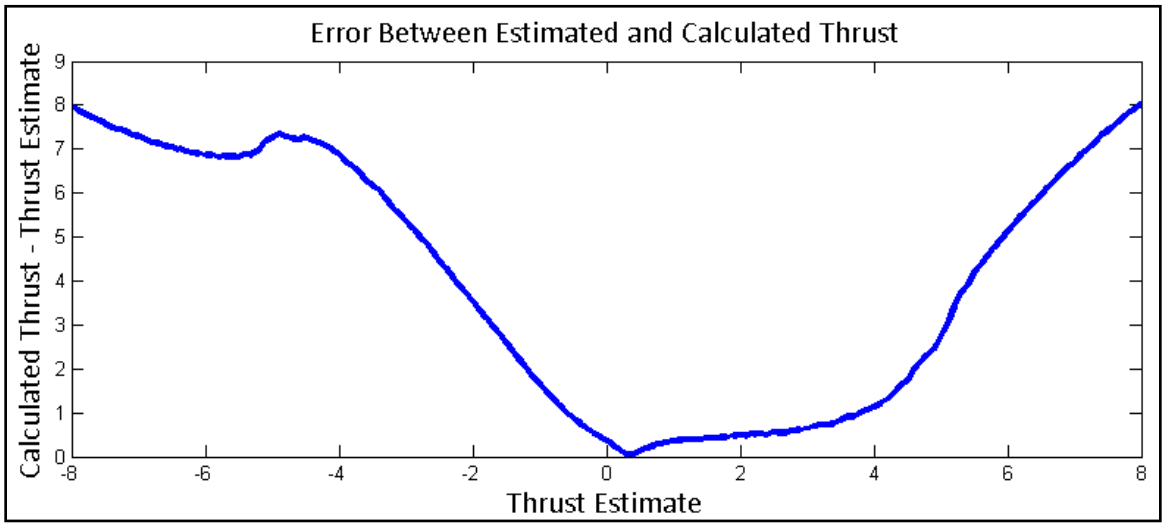

Figure 13. Convergence of thrust in BEMT loop.

In practical terms, this means that the BEMT analysis could converge upon the wrong thrust estimate. Therefore, it is currently necessary for the BEMT code user to exercise discretion when deciding upon the range of inputs for thrust estimation. This requires the user to have an idea of where the converged value should lie, e.g., experimental data can be used in conjunction with other methods of calculating thrust to search for a minimum near the correct location. In the future, a more robust optimization routine should be used that doesn't require the user to employ intuition about the "correct" range of inputs and outputs.

One main component of the project was to use 3-D wing scatter plots to calculate the lift coefficient of various wing airfoil slices along the span throughout the flapping cycle. In the BEMT code, airfoil shapes are analyzed at discrete points along the span, and thin airfoil theory is used to estimate C_l for the airfoil. Airfoil slices taken from the 3-D wing scatter plots at the root, mid-chord, and tip are shown in figure 14. The lines are a 3rd order polynomial approximation of the scatter coordinates, using the procedure shown in figure 11. Note that the

magnitude of curvature shown is a slight exaggeration due to the step size on the *z*-axis (max thickness is much smaller than shown). It is seen that the wing will be deformed both concave up and concave down along the span, and these deformations will change throughout the flapping cycle.

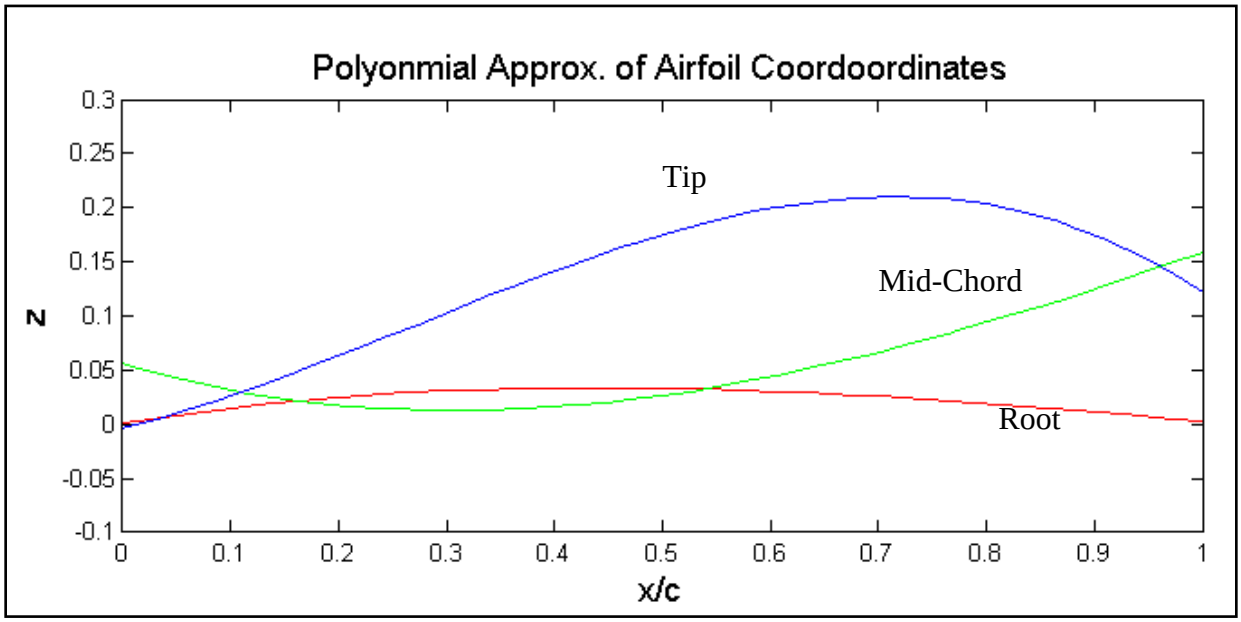

Figure 14. Wing airfoil approximations across the span.

3.2 3-D Wing Scatter Plot Airfoil Representation

Using the same airfoil shapes seen above for calculations in thin airfoil theory (figure 15), it is seen that the C_l versus α curve varies greatly for each of the airfoil shapes. Generally, more curvature when concave down will result in more positive values of C_l, as well as a higher value of zero lift angle of attack. This is reflected in figure 15, where the tip shape is the most concave down and produces the highest values of C_l, while the mid-chord shape (concave up) produces negative C_l values at most angles of attack. It is interesting to note the predicted C_l values at high angles of attack (AoA) (e.g., 15+), where the highest estimated value for the three airfoils shown is C_l ~3.4 at AoA = 20° (tip airfoil), and even the lowest predicted C_l at 20° is for the mid-chord airfoil, where C_l ~ 0.6. Because the RoboRaven cruises at AoA = 20°, it is likely that these high AoA C_l calculations using thin airfoil theory are overestimates (this is expanded upon later).

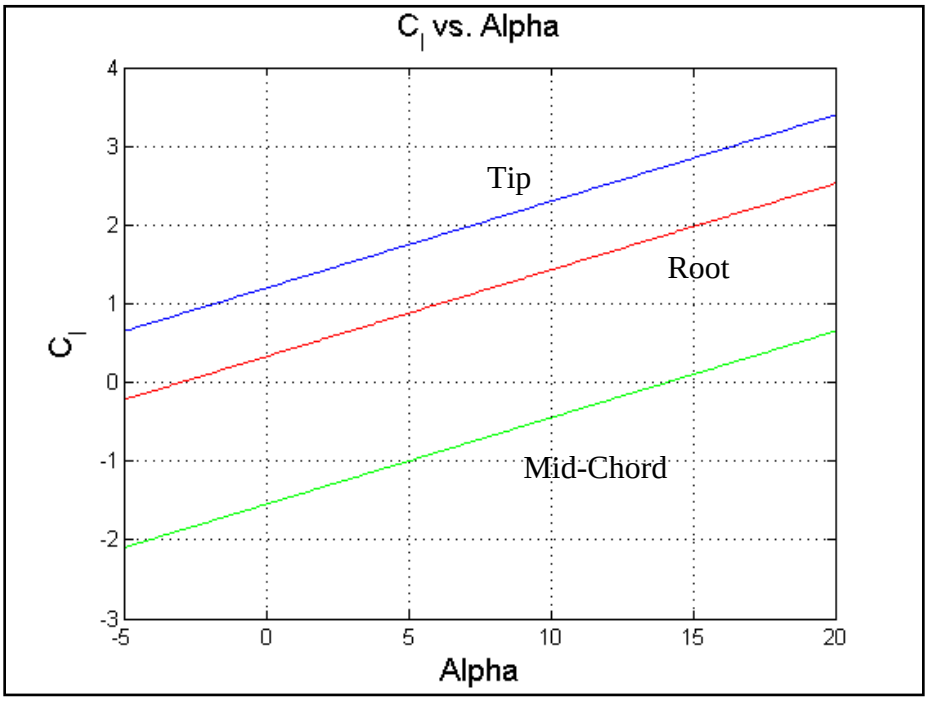

Figure 15. C_l vs. α curves across span.

3.3 BEMT Code Lift and Thrust Calculations

As lift and thrust are the two main forces analyzed in this project, one interesting comparison of the entire BEMT code (including wing scatter data) is the change in both thrust and lift versus AoA. This is shown in figure 16, When calculating thrust and lift versus AoA, the lift increases roughly linearly with AoA. This makes sense physically and analytically, because the lift coefficient was calculated using thin airfoil theory. The thrust change with AoA is nonlinear and appears to be relatively unpredictable through the range of AoAs shown. According to momentum theory, when a wing is placed at an increasing AoA, a correspondingly increasing amount of airflow will be deflected downward, thereby increasing lift. As this downward deflection increases (AoA increases), more airflow will be used for lift and less for thrust creation, thus thrust should generally decrease. Conversely, as AoA decreases into negative values, the wing flapping should move more air in the thrust plane. This concurs with figure 16, where thrust appears to reach a maximum at approximately AoA = –2°.

It is interesting to note that the BEMT thrust appears to remain relatively unchanged between ~2° < AoA < 12°. This differs greatly from the linear decrease in thrust from AoA = 12° to AoA = 25°. In comparison to the BEMT thrust, the DeLaurier-calculated thrust appears to be roughly parabolic, with a maximum thrust around AoA = 5°. For both the DeLaurier and BEMT calculations shown, the set of inputs were exactly the same, e.g., $\beta = 0°/m$ and the same 3-D wing scatter plots were used for wing shape throughout flapping.

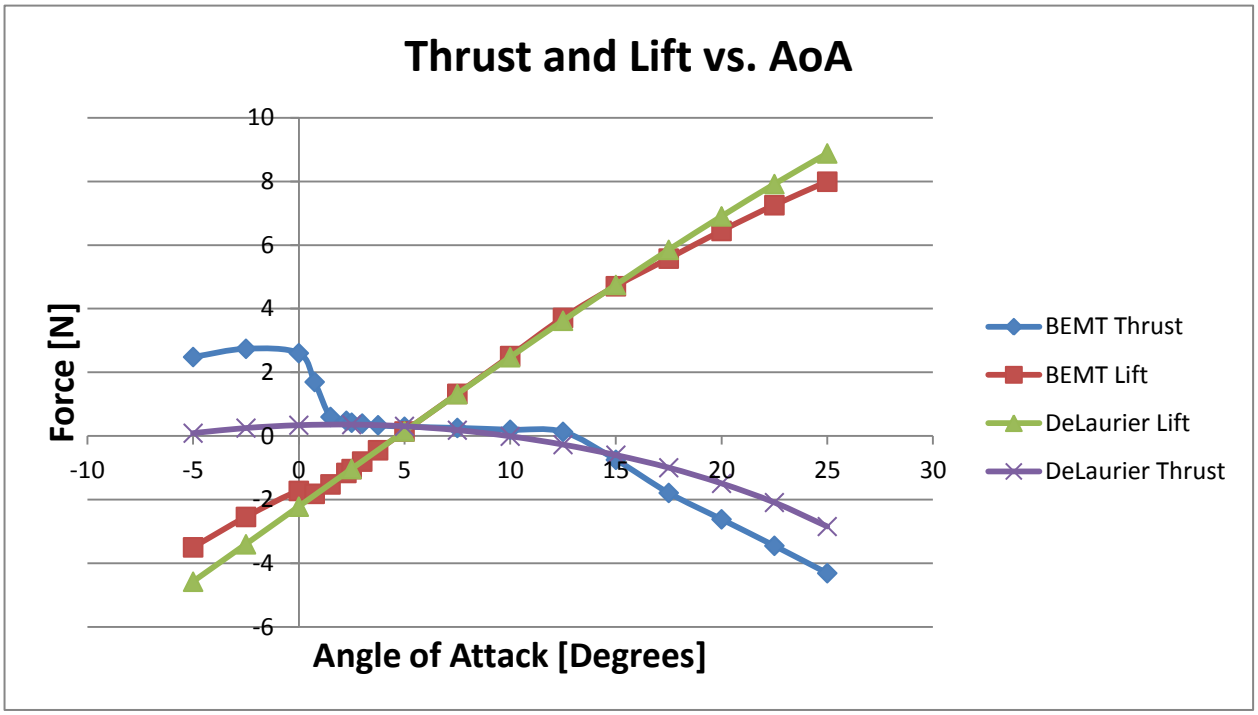

Figure 16. Calculated thrust and lift vs. AoA.

For the experimental wind tunnel measurements of the RoboRaven, it was found that average lift and thrust were 2.38 N and 1.14 N, respectively, when oriented at a 20° AoA in the wind tunnel. This AoA was chosen because the RoboRaven was measured to cruise in free flight at 20° with the horizontal free stream. The BEMT code calculates lift and thrust at 6.44 N and –2.62 N, respectively, for an input of AoA = 20° (table 1). It is likely that the lift is overestimated significantly because of the underlying limitations of thin airfoil theory. Thin airfoil theory calculates C_l as entirely linear regardless of AoA, whereas the stall region at high angles results in a sudden drop in C_l.

Table 1. Lift and thrust for $\beta = 0$, $\alpha = 20°$.

	Experimental Measurements	**BEMT Calculations**	**DeLaurier BET**
Average lift [N]	2.38	6.44	6.90
Average thrust [N]	1.14	–2.62	–1.50

Comparing these experimental measurements with figure 16 showing BEMT calculated thrust and lift over a range of AoAs, the closest match between these forces is at AoA = 10°, where lift = 2.51 N and thrust = 0.20 N. Lift calculation via thin airfoil theory appears to be an

overestimate at high AoAs, since the actual RoboRaven wind tunnel measurements were performed at AoA = 20° and match the BEMT thrust calculations at AoA = 10°. Additionally, the BEMT code significantly underestimates thrust, especially at high AoAs. The thrust estimation at AoA = 20° is much lower than the experimental results, especially when comparing the BEMT results to the original DeLaurier BET results. It is seen that the DeLaurier BET is more positive at AoA = 20°, but is still very different from the experimental measurement (Thrust = –1.5 N for DeLaurier vs. 1.14 N experimentally). It is clear that thrust effects are not being accounted for in both DeLaurier and the BEMT model, which are causing both to underestimate thrust at higher AoAs.

4. Summary and Conclusions

The initial goals of this project were to improve upon existing aerodynamic models for FWUAVs by implementing BEMT and more accurately depict wing shape in flight by using experimental wing deformation measurements. The first goal was accomplished by combining J.D. DeLaurier's BET model with Shkarayev's momentum theory model and iterating on induced velocity to converge on thrust between the two models. The second goal was accomplished through the use of experimentally obtained 3-D scatter plots of the FWUAV wing shape throughout the flapping cycle. Many observations and conclusions can be drawn from the general methodology used in this project, as well as on the specific method used for implementation.

The main reason for implementing a BEMT analysis is that convergence between two different calculation methods and using momentum theory for induced velocity calculation will yield a more accurate final result. However, scrutiny must still be given to the original BET and momentum theory models that were combined to create the BEMT model, as each model will still have individual limitations. In this project, the DeLaurier BET model approximates wing flapping motion as generally sinusoidal, with inputs such as flapping angle, flapping frequency, and wing geometric. While this general method does resemble actual flapping in its periodic motion, the 3-D scatter plots from DIC data used in this project can be used to more accurately represent wing flapping shapes. Because wing shape is very important when calculating lift and thrust, further improvements to wing flapping motion modeling should be made. DIC can be used to measure wing flapping velocity and acceleration; creating function regressions from these DIC measurements could be used in place of purely sinusoidal motion. Ideally, this would enable the aerodynamic model to have a coupling between both wing deformation and motion to be used in BEMT calculations.

Similarly, the Shakarayev model used in this analysis was relatively simple, as described in section 3, since flow properties are assumed to be uniform throughout the entire disk area. Because flight forces across the wing vary greatly with wing shape and speed (tip speeds are higher than root speeds), an improved momentum model would account for these differences across the span. This approach has been used for rotorcraft, where both models are functions of geometric properties, as well as spanwise location along the rotor blades.

Another main component of the project was to use thin airfoil theory to approximate the lift coefficient across the wing throughout the flap cycle. While distinct in its approach (the original DeLaurier BET model does not use experimental wing shape measurements), the resulting lift coefficient calculations seem to largely overestimate the true wind tunnel load cell measurements. This is attributed to the ideal nature of thin airfoil theory—thin airfoil theory calculates a purely linear C_l versus α curve, which means the user could technically input an extremely large, unrealistic AoA (e.g., AoA = 50°) and thin airfoil theory would calculate a correspondingly high C_l with no stall effects included. Thus, while the usage of DIC wing shape measurements is one step toward a better approximation of lift coefficient for a flapping wing, it would be beneficial to improve the high AoA C_l calculations. While it is possible that the actual lift coefficient at high AoAs for the most concave portions of the wing truly are in the neighborhood of C_l = 3–4, it is unlikely. Better accounting for separation effects at high AoA (where many FWUAVs fly) should be a focus in the future.

The final goal of this project was to improve the thrust estimation within the BEMT code. When comparing the BEMT results with the experimental wind tunnel results at AoA = 20°, it was found that the BEMT code significantly underestimates thrust at higher AoAs. The exact reason why this is occurring has not yet been defined; however, the DeLaurier BET code's function approximation of thrust (which the BEMT code is based on) appears to underestimate thrust and overestimate lift. It is believed the code should be modified for these issues (this project does not explore how to fix the problems), such that the forces on an airfoil section better estimate the thrust generated. Since the BEMT code was created as an attempt to improve thrust calculation, it appears the specific BEMT method used in this project should be improved further since the thrust is underestimated more than when using the original DeLaurier BET code. One possible cause is that the Shkarayev momentum theory approximates the partial disk area created by wing flapping as having uniform flow properties. In reality, since the flow changes significantly along the wing span, these changes need to be accounted for in momentum theory. This type of momentum theory, which is based on the radial/spanwise location, has been used in rotorcraft theory for decades (see Leishman [*8*]), and an adaptation for flapping wings could prove beneficial.

5. References

1. Aerovironment, Inc. www.avinc.com (accessed 31 July 2013).
2. *Young Australian at the Forefront of UAV Innovation*. (2009, August). Retrieved 2013, from Australian Government Defense Materiel Organisation: http://www.defence.gov.au/dmo/news/ontarget/2009/jul09/inn.cfm (accessed 31 July 2013).
3. Lehman, F.; Pick, S. The Aerodynamic Benefit of Wing–Wing Interaction Depends on Stroke Trajectory in Flapping Insect Wings. *J. of Experimental Biology* **2007**, *210*. http://jeb.biologists.org/content/210/8/1362.full.pdf+html.
4. University of Maryland, http://youtu.be/mjOWpwbnmTw (accessed 31 July 2013).
5. DeLaurier, J. D. An Aerodynamic Model for Flapping-Wing Flight. *Aeronautical Journal* **1993**, Institute of Aerospace Studies, Ontario.
6. Shkarayev, S.; Silin, D. Applications of Actuator Disk Theory to Membrane Flapping Wings. *AIAA Journal* **October 2010**, *48* (10).
7. Anderson, J. *Fundamentals of Aerodynamics*; McGraw-Hill Inc.: New York, 1984.
8. Leishman, J. G. *Principles of Helicopter Aerodynamics*. Cambridge University Press. 2006.

1 DEFENSE TECHNICAL
(PDF) INFORMATION CTR
DTIC OCA

1 GOVT PRINTG OFC
(PDF) A MALHOTRA

2 DIRECTOR
(PDF) US ARMY RESEARCH LAB
RDRL CIO LL
IMAL HRA MAIL & RECORDS MGMT

1 DIRECTOR
(PDF) US ARMY RESEARCH LAB
RDRL VTV J GERDES